SHEARING STRESSES AND SURFACE DEFLECTIONS DUE TO TRAPEZOIDAL LOADS

By D. L. Holl

Professor of Mathemetics, Iowa State College

SYNOPSIS

In this paper the stresses and surface deflections of a semi-infinite elastic medium, and of an elastic layer of finite depth are obtained by the principle of superposition. When these effects are known for a concentrated surface load, the corresponding results for distributed or continuous surface loads may be obtained by summation or integration methods.

In the first part of the paper the author determines all the stresses in the supporting medium for surface loads which simulate triangular, symmetrical and unsymmetrical trapezoidal surface loads due to road fills, and determines the maximum shearing stresses under such loads. In particular it is shown that the depth at which this maximum shear occurs under a symmetrical trapezoidal fill is at a depth approximately equal to one-half of the length of an equivalent rectangular load of equal intensity. This maximum shear value does not exceed 0.318 p where p is the maximum intensity of the surface loading.

In the second part of the paper, superposition methods are employed to determine the stresses and surface deflection of a finite elastic layer supported by a rough rigid base, and bearing a trapezoidal surface load. It is shown that the stresses are no longer independent of Poisson's ratio ν, and that shearing failure occurs within the layer before it occurs at the supporting base. The surface deflections are evaluated (using $\nu = 0.25$) for several types of surface loading and varying depths of the elastic layer. It is also shown that the results of the first part of the paper can be derived as a limiting case by allowing the depth of the layer to become infinite.

It is recognized that these solutions furnish basic pictures, departures from which in the imperfectly elastic material must be examined and judged by experimental progress.

It is a common observation that the theory of elasticity is useful beyond the range of only those media which, in the true sense, are purely elastic. Thus, soil mechanics, which deals with materials that are far from being perfectly elastic has profited from the results of classical theory for the transmission of surface pressures in a supporting medium. These solutions only furnish basic pictures, departures from which in the imperfectly elastic material must be examined and judged by experimental progress.

In this paper the analytical method of Boussinesq, assuming plane strain conditions, is applied to two dimensional problems for the determination of the distribution of the stresses and the surface displacements of a semi-infinite elastic medium bearing surface loads. By a plane strain or plane deformation problem is meant a stressed body which is very long in one direction in comparison with the other transverse dimensions, so that the stresses and deformations are the same in all transverse sections. It is also assumed that the supporting medium has uniform elastic properties, and that the resulting distribution is due to the surface loads and not to the body forces of the supporting medium.

In the paper, two cases are considered: Case (a), The supporting medium is infinitely deep and has a horizontal surface plane,[1] Case (b), The medium is an elastic layer of finite depth h with a horizontal surface plane, and resting on a rough rigid base.

[1] In the appendix the case of an inclined surface plane is treated. These results were appended at the suggestion of Dr. Karl Terzaghi whose written discussion was presented to the writer.

In both cases the chief consideration is to ascertain (1) the distribution of stresses and (2) the surface deflections. In particular the author determines the principal shearing stresses under symmetrical surface loads whose intensity is indicated by the trapezoidal loadings of Figures 2 and 8. If one may assume that this loading simulates a road fill on a naturally horizontal earthy medium, then the results may indicate the nature of the stress distribution. No assertion is made that the results hold in such an imperfectly elastic medium. The analysis is more likely to hold for the stress distribution than for the surface deflections.

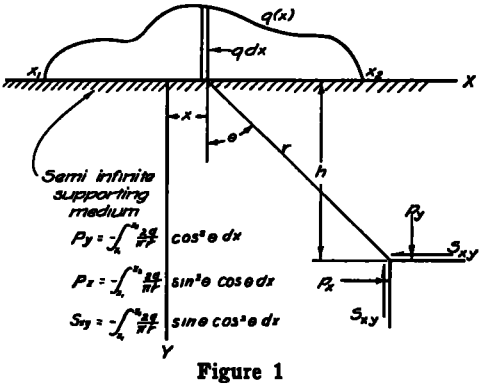

Figure 1

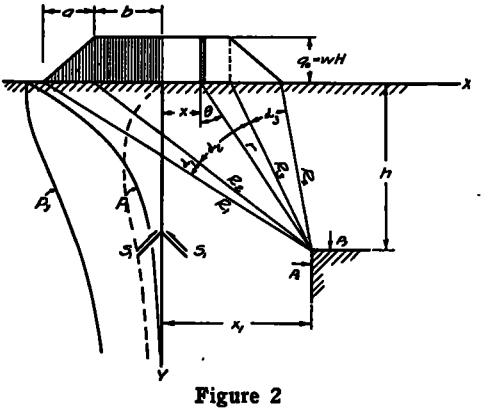

Figure 2

STRESSES IN A SEMI-INFINITE MEDIUM

Consider a case of plane deformation where a loading q(x) in Figure 1 produces stresses and deformations in the supporting medium. From the elastic theory of Boussinesq one deduces the stresses p_x, p_y, and S_{xy} from the following integrals (the coordinates and elements are shown in Fig. 1).

$$p_x = -\int_{x_1}^{x_2} \frac{2q(x)}{\pi r} \sin^2\theta \cos\theta \, dx,$$

$$(1) \qquad p_y = -\int_{x_1}^{x_2} \frac{2q(x)}{\pi r} \cos^3\theta \, dx,$$

$$S_{xy} = -\int_{x_1}^{x_2} \frac{2q(x)}{\pi r} \cos^2\theta \sin\theta \, dx.$$

In Eqs. (1), the integrands are the stresses for an elemental loading q dx. By employing summation or integration for discrete or continuous loads, the stresses on elements at $x = x_1$ and at depth $y = h$ may be obtained. The results for the symmetrical trapezoidal loading of Figure 2 have been given by Palmer.[2] Slightly more general results are given for the case of Figure 3a where the central trapezoidal loading has two additional triangular loads of the same slope. These stresses are

$$p_y = -\frac{q_0}{\pi}\left[\left(\alpha_1 + \frac{\alpha_2}{2}\right) + \frac{b}{a}(\alpha_1 + \alpha_3) + \frac{x_1}{a}(\alpha_1 - \alpha_3) - \frac{x_1\alpha_2}{2b}\right] - \frac{q_1}{\pi}\left(\alpha_3 + \frac{\alpha_2}{2} + \frac{x_1\alpha_2}{2b}\right),$$

$$(2) \quad p_x = p_y - \frac{2q_0h}{\pi a} \log\frac{R_2R_3}{R_1R_4} - \frac{(q_1 - q_0)h}{\pi b} \log\frac{R_3}{R_2},$$

$$S_{xy} = \frac{hq_0}{\pi a}(\alpha_1 - \alpha_3) + \frac{(q_1 - q_0)h\alpha_2}{2\pi b},$$

[2] Palmer, L. A., "Principles of Soil Mechanics Involved in the Design of Retaining Walls and Bridge Abutments," *Public Roads*, Vol. 19, pp. 193-207, 1938.

where a_1, a_2, and a_3 are the angles subtended at the point in the supporting medium by the loading. The constants q_0 and q_1 are indicated intensities of the loading. The distances R_1, R_2, R_3, and R_4 in Figure 3a correspond to similar distances shown in Figure 2.

shows that there is an equal compressive stress or hydrostatic pressure directly under a normal surface loading. Another important observation is that all the stresses are independent of the elastic moduli of the supporting medium. Neither of these last two statements hold

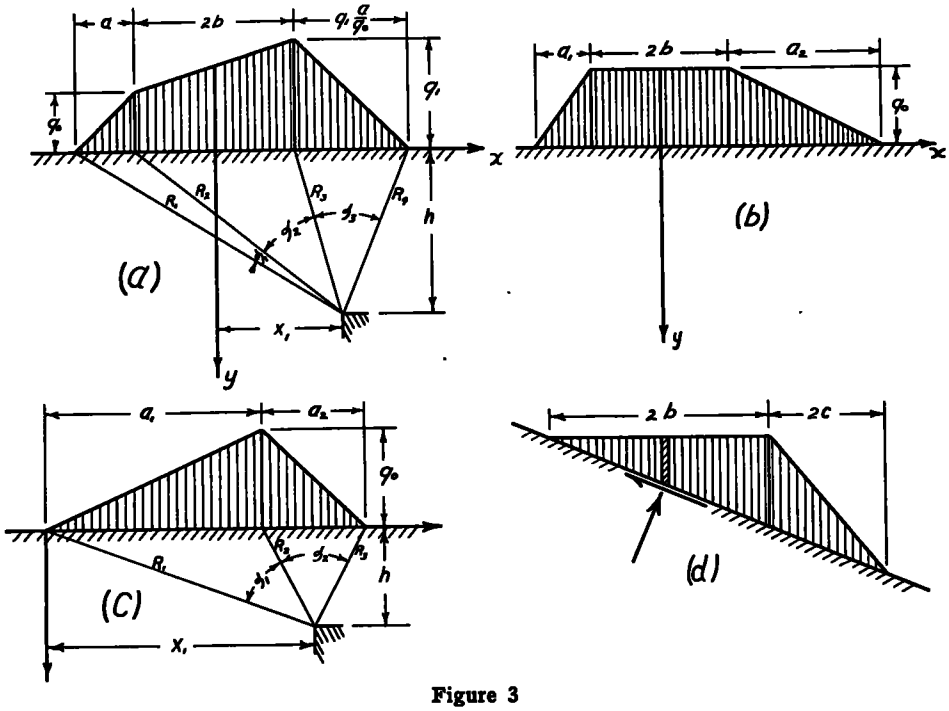

Figure 3

An examination of Eqs. (2) shows that when $h=0$, the shearing stress $S_{xy}=0$, that is, there is no tangential loading on the top surface. Also $p_x=p_y$ when $h=0$, for the finite layer problem treated in the latter part of this paper.

For the unsymmetrical trapezoidal loading of Figure 3b, these stresses are

$$p_y=-\frac{q_0}{\pi}\left[(a_1+a_2+a_3)+\frac{b}{a_1}(a_1+ka_3)+\frac{x_1}{a_1}(a_1-ka_3)\right],$$

$$p_x=p_y+\frac{2q_0}{\pi}\left[\frac{h}{a_2}\log R_4/R_3-\frac{h}{a_1}\log R_1/R_2\right], \tag{3}$$

$$S_{xy}=\frac{q_0 h}{\pi a_1}(a_1-ka_3),$$

and outside the loading area, where $a_1=a_2=a_3=0$, $p_x=p_y=0$. Under the loading $p_x=p_y=$unit load applied. This where the constant $k=a_1/a_2$ is the ratio of the projections of the sloping sections. The comments concerning Eqs. (2) hold

for Eqs. (3). If $k=1$ in Eqs. (3) or if $q_1=q_0$ in Eqs. (2) the stresses reduce to the results given by Palmer for a symmetrical trapezoidal load. For the triangular loading of Figure 3c the results may be obtained from Eqs. (3) by letting b approach zero, $a_2=0$ and $R_2=R_3$, that is (with a_3 becoming a_2),

$$
\begin{aligned}
p_y &= -\frac{q_0}{\pi}\left[\frac{a_1 x_1}{a_1} + a_2(1+a_1/a_2-x_1/a_2)\right],\\
p_x &= p_y + \frac{q_0}{\pi}\left[\frac{2h}{a_1}\log R_2/R_1 - \frac{2h}{a_2}\log R_3/R_2\right], \qquad (4)\\
S_{xy} &= \frac{q_0 h}{\pi}(a_1/a_1 - a_2/a_2).
\end{aligned}
$$

Many additional special cases could be obtained such as a rectangular loading (by allowing $a_1=a_2=0$ in Eqs. (3)), or a trapezoidal loading such as the central portion of Figure 3a (by allowing $a=0$ in Eqs. (2)), or an infinitely long embankment loading when $a_2=\infty$ in Figure 3c. All the above results have been derived by superposition methods upon the assumption that the loads exert only a normal pressure upon the supporting medium. Figure 3d indicates a case where the load is supported by a medium whose surface is not perpendicular to the gravitational field which is taken to be vertical. In this case the surface loading exerts a normal as well as a tangential stress upon the inclined surface of the supporting medium. The stresses for this type of loading are included in the appendix.

MAXIMUM SHEARING STRESSES

Again considering the special case of Figure 2, one finds the greatest shearing stresses occur on the vertical axis under the symmetrical loading. Since the shearing stress S_{xy} vanishes on this axis, the normal stresses p_x and p_y are principal stresses (these curves are shown with a lateral scale which has a value of q_0 at the surface). Hence on elements inclined 45° with this vertical axis, the principal shearing stress S_1 is one-half the difference of these normal stresses (Fig. 2 shows this S_1 stress by a broken line),

$$S_1 = \frac{p_y - p_x}{2} = \frac{2q_0 h}{\pi a}\log R_1/R_2 = \frac{q_0 h}{\pi a}\log\frac{h^2+(a+b)^2}{h^2+b^2}. \qquad (5)$$

The depth $\bar{h}$, at which this shearing stress becomes a maximum depends on the dimensions a and b of the loading. This value of $\bar{h}$ is a solution of the equation

$$\frac{2h^2(a^2+2ab)}{(h^2+b^2)[h^2+(a+b)^2]} = \log\frac{h^2+(a+b)^2}{h^2+b^2}.$$

Some special values are as follows:

When:		Then:		
	$a=0.0b$		$\bar{h}=1.00b$,	$S_1=0.318q_0=q_0/\pi$
	$a=0.5b$		$\bar{h}=1.24b$,	$S_1=0.316q_0$
	$a=1.0b$		$\bar{h}=1.48b$,	$S_1=0.314q_0$
	$a=2.0b$		$\bar{h}=1.92b$,	$S_1=0.310q_0$.

If one may assume for the sake of an application of these results, that the loading of Figure 2 is an actual road fill of height H with the slope fills depending upon H, then if the loading intensity is proportional to the height, the critical depth $\bar{h}$ depends upon H as well as the dimensions of the loaded regions. In Tables 1 and 2 accurate values of $\bar{h}$ and

the corresponding S_1 stresses are given for a range of values of b and H, with variable sloping fills and differing densities of loading materials.

One observes that if a symmetrical trapezoidal loading is replaced by a rectangular load of length $2b+a$, then the critical depth is $\bar{h}=b+a/2$ and S_1 has a maximum value of $0.318q_0$. These values are only slightly greater than the corresponding values of Tables 1 and 2. Thus a reasonably safe field rule is to investigate the shearing capacity of the supporting layer at a depth approximately equal to half the length of equivalent rectangular load.

TABLE 1

VALUES OF $\bar{h}$ FOR VARIOUS ROADWAYS, SLOPES AND HEIGHTS OF FILL

H ft.	1.5 to 1 slope			1.65 to 1 slope			1.8 to 1 slope		
	Roadway =2b			Roadway =2b			Roadway =2b		
	32 ft.	36 ft.	40 ft.	32 ft.	36 ft.	40 ft.	32 ft.	36 ft.	40 ft.
10	23	25	27	24	26	28	24	26	28
20	30	32	34	31	33	35	33	35	37
30	37	39	41	39	41	43	41	43	45
40	44	46	48	46	48	50	49	51	53
50	50	52	54	54	56	58	57	59	61
60	57	59	61	62	64	66	66	68	70
70	64	66	68	69	71	73	74	76	78
80	71	73	75	77	79	81	82	84	86
90	78	80	82	84	86	88	91	93	95
100	85	87	89	92	94	96	99	101	103

TABLE 2

SHEAR STRESS IN LB. PER SQ. FT. FOR VARIOUS HEIGHTS OF FILL AND UNIT WEIGHT OF FILL MATERIAL

H ft.	110 lb. per cu. ft.	120 lb. per cu. ft.	130 lb. per cu. ft.
10	341	372	403
20	682	744	806
30	1,023	1,116	1,210
40	1,364	1,488	1,612
50	1,705	1,862	2,016
60	2,046	2,231	2,419
70	2,387	2,602	2,820
80	2,728	2,975	3,223
90	3,069	3,348	3,627
100	3,410	3,720	4,030

SURFACE DEFLECTION IN A SEMI-INFINITE MEDIUM

One may apply the superposition method to find the surface deflection on an elastic medium due to distributed loads if the deflection for a point load is known. From the classical elastic theory [3] only the relative deflection of this surface can be derived. Some point whose deflection is taken as zero must be chosen as a reference point, and all deflections are then referred to this point. For convenience it may be chosen as a point interior to the supporting medium, or upon the top surface. In this paper it is expedient to choose this reference point as some point on the top surface and external to the loaded area. Since this problem is one of plane displacement, it appears that a reference point in the surface admits of experimental observation.

[3] Timoshenko, S., "Theory of Elasticity," pp. 86-88. His case is the case of plane stress and all deflections are made relative to a reference point on the vertical axis at which the deflection vanishes.

In Figure 4 the surface deflection relative to a point d due to an elemental surface loading q dx is

$$(6)\quad w(x) = 2q\,dx\frac{(1-\nu^2)}{\pi E}\log\frac{d-x_1}{|x-x_1|},$$

where x_1 is the abscissa of the loading element, E the compression modulus and ν is the Poisson's ratio of the supporting

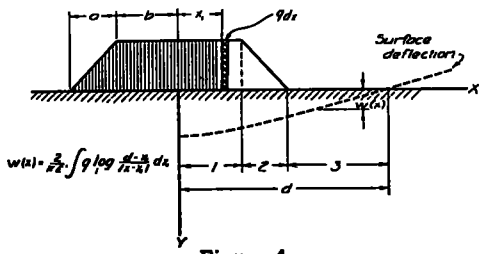

Figure 4

medium. The distance d is measured from the origin. It is a surface point at which the deflection vanishes and relative to which all interior deflections are measured. There is nothing in the analysis by which this value can be found. It is an indeterminate [4] and the results are not valid beyond this value of d.

For the trapezoidal loading, Figure 4 which has discontinuities in the slopes, the integration leads to three different forms of the deflection expressions. These may be denoted by w_1, w_2, and w_3 and are valid in the regions 1, 2, and 3 respectively of Figure 4. However all three may be written by a single expression if absolute values are used in the logarithmic terms.

$$(7)\quad w(x) = 2q/\pi E'\left[K + \frac{b^2+x^2}{2a}\log\frac{|x^2-b^2|}{|x^2-(a+b)^2|} + bx/a\log\frac{x+b}{|x-b|} + \frac{x(a+b)}{a}\log\frac{|a+b-x|}{a+b+x} + (b+a/2)\log\frac{d^2-(a+b)^2}{|x^2-(a+b)^2|}\right],$$

where

$$K = (b^2+d^2)/2a\log\frac{d^2-(a+b)^2}{d^2-b^2} + bd/a\log\frac{d-b}{d+b} + \frac{d(b+a)}{a}\log\frac{d+a+b}{d-a-b},$$

and

$$E' = E/(1-\nu^2).$$

The constant K depends only on the dimensions of the loaded region and the value of d. Each term of Eq. (7) contains a natural logarithm of a dimensionless ratio, and hence the bracketed expression is of the same dimension as b or a. One notes that the elastic moduli of the supporting medium appear only in the leading factor $2q/\pi E'$ which is dimensionless. Apart from this factor the elastic deflection of the top surface is not influenced by the type of the elastic supporting medium. Since the leading factor is purely a scale factor, it may be said to be a "foundation modulus" [5] and capable of experimental determination.

Equation (7) may be written out for each of the three regions and a continuous deflection curve drawn for selected ratios of d/a and d/b such as shown in Figures 5a and 5b. One notes that for a fixed value of d these curves do not cross each other except at the reference point d where the deflection vanishes. With increasing loading areas

[4] While d appears as an integration constant, it is not possible to assume that the deflection vanishes at infinity, for then all the displacements near the finite loading become infinite. M. A. Biot has indicated this in a plane stress problem in *Journal of Applied Mechanics*, Vol. 4, No. 1, pp. 1-7, 1937.

[5] In an elastic medium whose moduli are known, the quantity $E' = E/(1-\nu^2)$ is also known. Assuming the possibility of an application to a field experiment with the earth as a supporting medium, this foundation modulus and the value of d admit of an actual determination by two deflection readings. Even in an ideal medium, the value of d must be obtained by experiment.

(having a fixed maximum intensity q) the maximum deflection increases. This is more evident in Figure 6 where the maximum central deflection is shown for a range of ratios of a/b and d/b. From Eq. (7) this maximum deflection is

(8) $$w(0) = 2q/\pi E' \left[K + (2b+a)/2 \log \frac{d^2-(a+b)^2}{(a+b)^2} + b^2/a \log \frac{b}{a+b} \right].$$

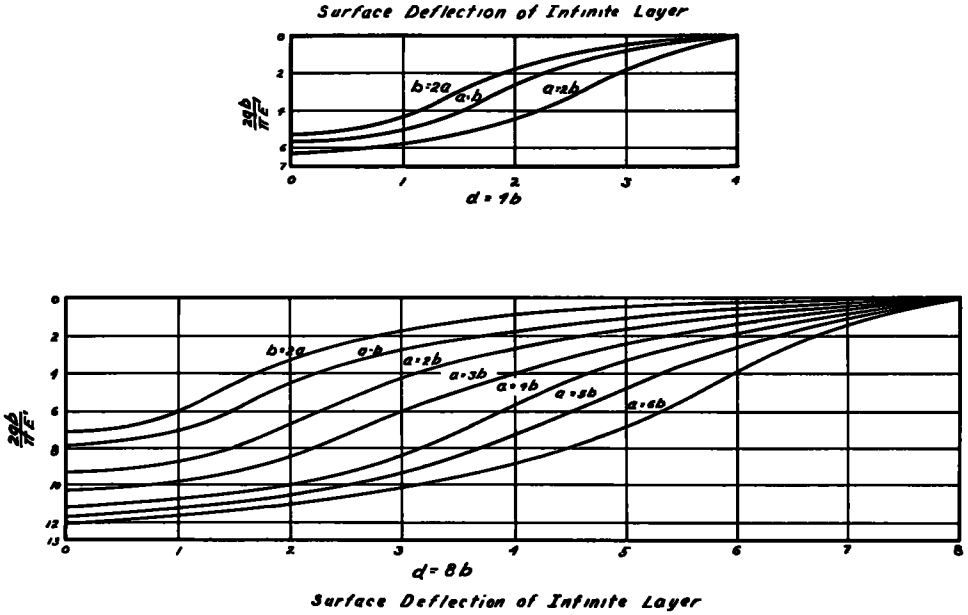

Figure 5

From Figure 6 one is lead to the conclusion that as d increases indefinitely the deflection in the finite portions of the plane also increases beyond bound. This fact will be referred to in the analysis of the problem of an elastic layer of finite depth.

STRESSES IN A FINITE ELASTIC LAYER

In Figure 7 is shown an elastic layer of finite depth h supported on a rough rigid base. The surface loading is F(x). Again the assumption is made that all transverse sections are under the same force systems and the problem is one of plane deformation. There is considerable literature available regarding this and related problems. Carothers[6] gave an incorrect solution for this case. Timoshenko objected to Carothers' solution by oral discussion at the time, but the error was not generally known until recently.[7] The first correct solution for the plane stress case was given by Marguerre.[8] It can be shown that the results of this

[6] Carothers, S. D., *Proceedings*, Int. Math. Congress, Vol. 2, Toronto, Canada, 1924.

[7] L. Jurgenson, *Journal*, Boston Society of Civil Engineers, Vol. 21, 1934 and in *Proceedings*, International Conference on Soil Mechanics, Vol. 2, 1936, derives formulas for other loadings by assuming Carothers' incorrect results. W. Passer, in Sitz. B. Akad. Wiss. Wien, Vol. 144, pp. 267, 1935, first gave the correct solution of the axially symmetric case on a rough base and refers to Carothers' error.

[8] Marguerre, K., in *Ing. Archiv*, Vol. 2, pp. 108-117 (1931) gives the plane stress case on a rough base, and in *Ing. Archiv*, Vol. 4, pp. 332-353 (1933) treats the axially symmetric case on a rough base or a yielding base.

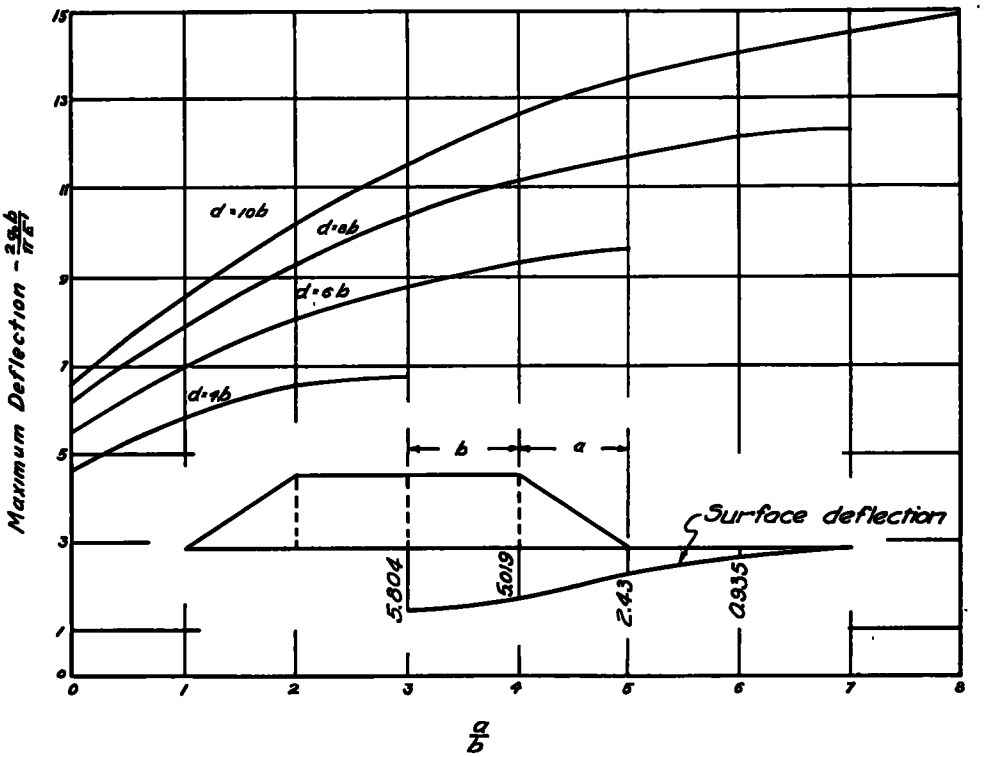

Figure 6

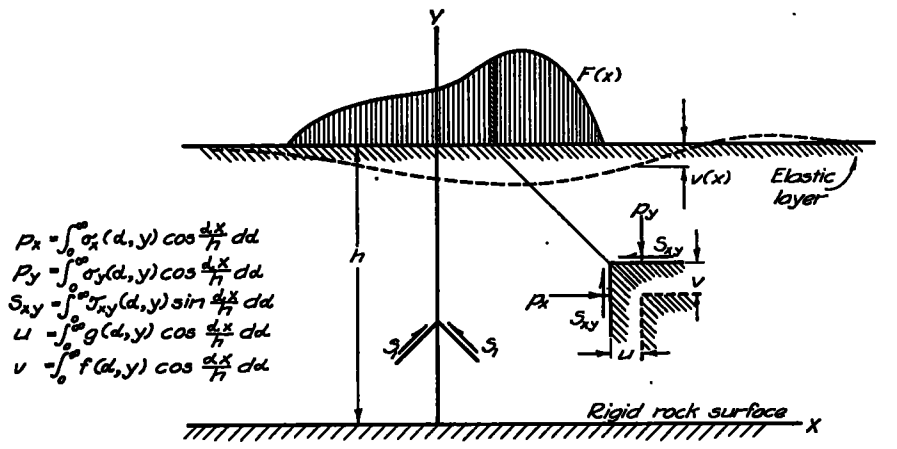

Figure 7

paper are derivable from his results by the usual transition from plane stress to plane deformation. Biot [9] has solved the problem correctly not only for plane deformation but also for the axially symmetric case for the special value of Poisson's ratio $\nu=0.5$. More recently and quite unknown to the writer, Pickett [10] has considered both the plane strain and the axially symmetric case. The immediate interest of the present paper was to consider the relationship of the maximum shearing stresses under the center of a symmetrical trapezoidal loading with the shearing stresses at the rough base, and to find the surface deflections.

Let the coordinate system be that of Figure 7. The conditions at the rock base where $y=0$ are that the horizontal and vertical displacements (u, v) shall vanish. At the surface $y=h$, the shear, $S_{xy}=0$ and p_y is the loading. Hence

$$(9) \qquad [u]_{y=0}=[v]_{y=0}=0;\ [S_{xy}]_{y=h}=0;\ [-p_y]_{y=h}=\text{loading}.$$

Now one seeks to find a stress function ϕ satisfying the biharmonic equation $\nabla^4\phi=0$ such that all the boundary conditions of Eqs. (9) are satisfied. For symmetrical normal surface loads which are finite in the neighborhood of the origin, a suitable stress function is

$$(10) \qquad \phi=\int_0^\infty [A\cosh ay+B\sinh ay+Cay\cosh ay+Day\sinh ay]\cos ax\,da$$

where A, B, C, and D are constants to be determined. One may formulate the boundary conditions in Eq. (9) by the relationships

$$p_x=\phi_{yy};\ p_y=\phi_{xx};\ S_{xy}=-\phi_{xy},$$

$$(11) \quad Eu=\int[(1-\nu^2)\phi_{yy}-\nu(1+\nu)\phi_{xx}]\,dx,$$

$$Ev=\int[(1-\nu^2)\phi_{xx}-\nu(1+\nu)\phi_{yy}]\,dy.$$

The first three conditions of Eqs. (9) lead to

$$B=(1-2\nu)C=\frac{A(1-2\nu)}{2(1-\nu)}\left[\frac{ah\cosh ah-(1-2\nu)\sinh ah}{ah\sinh ah+(1-\nu)2\cosh ah}\right] \qquad (12)$$

$$D=\frac{-A}{2(1-\nu)}.$$

To determine A, it is convenient to express the symmetric loading by the Fourier integral

$$F(x)=2/\pi\int_0^\infty\cos ax\,da\int_0^\infty F(\lambda)\cos a\lambda\,d\lambda$$

$$=\int_0^\infty Q(a)a^2\cos ax\,da$$

where

$$(13) \quad a^2Q(a)=2/\pi\int_0^\infty F(\lambda)\cos a\lambda\,d\lambda.$$

Now the last of Eqs. (9) and the definition of $p_y=\phi_{xx}$ lead to the condition

$$Q(a)=A\cosh ah+B\sinh ah+Cah\cosh ah+Dah\sinh ah$$

with B, C, and D given by Eqs. (12) and $Q(a)$ by Eq. (13) for any symmetrical loading. Accordingly one has

$$A=[2Q(a)/\Delta](1-\nu)[ah\sinh ah+2(1-\nu)\cosh ah], \qquad (14)$$

where

$$\Delta=(3-4\nu)\cosh^2 ah+(1-2\nu)^2+a^2h^2.$$

This completes the determination of the constants. Some special values of stresses p_x, p_y, and S_{xy} will be recorded. The general values of these stresses do

[9] Biot, M. A., *Physics*, Vol. 6, pp. 367-375 (1935).

[10] Pickett, G., in *Proceedings*, Highway Research Board, Vol. 2, pp. 35-48, 1938 has extended Biot's work for the rough rigid base. In private correspondence, Professor Pickett

not concern us at present, although it may be shown that they reduce to known results [11] when the value of h becomes infinite. In fact the limiting process shows that only in the infinite layer do the stresses become independent of Poisson's ratio.

The following are special values of the stresses.

(15)

$$p_x\Big|_{y=0} = -\int_0^\infty \frac{Q(a)}{\Delta}\,[2\nu a h \sinh ah + 4\nu(1-\nu)\cosh ah]\,a^2\cos ax\,da,$$

$$S_{xy}\Big|_{y=0} = -\int_0^\infty \frac{Q(a)}{\Delta}\,2(1-\nu)\,[ah\cosh ah - (1-2\nu)\sinh ah]\,a^2\sin ax\,da,$$

$$p_y\Big|_{y=0} = -\int_0^\infty \frac{Q(a)}{\Delta}\,[2(1-\nu)ah\sinh ah + 4(1-\nu)^2\cosh ah]\,a^2\cos ax\,da,$$

$$S_1\Big|_{x=0} = \int_0^\infty \frac{Q(a)}{\Delta}\Big\{(1-2\nu)\,[ah\sinh ah + 2(1-\nu)\cosh ah]\cosh ay$$
$$+2(1-\nu)\,[ah\cosh ah - (1-2\nu)\sinh ah]\sinh ay$$
$$+\,[ah\cosh ah - (1-2\nu)\sinh ah]\,ay\cosh ay$$
$$-\,[ah\sinh ah + 2(1-\nu)\cosh ah]\,ay\sinh ay\Big\}a^2\,da.$$

These equations give the stresses at the rough base and the principal shearing stress under the center of a symmetrical loading. In order to evaluate these stresses for any particular load, it is necessary to find $Q(a)$ from Eq. (13). For the trapezoidal loading of Figure 8, one finds from Eq. (13)

$$(16)\quad Q(a) = \frac{-2q}{\pi a b a^4}\,[\cos a(a+b) - \cos ab].$$

By allowing a to become zero, or b to vanish, one has

$$(17)\quad Q(a) = \frac{2q}{\pi a^3}\sin ab,$$

$$(18)\quad Q(a) = \frac{2q}{\pi a b a^4}\,[1-\cos aa].$$

Equation (18) represents an isosceles triangular loading and Equation (17) represents a rectangular loading, a special case being a point load P at the origin, namely,

$$Q(a) = P/\pi a^2.$$

Using Eqs. (16) and (15) a typical set of stress curves are shown in Figure 8. In Figure 9 one may make a comparison between the maximum shear stresses S_1 which occur on elements inclined at 45° with the vertical axis of symmetry (see Fig. 7) and the shearing stresses at the rock surface. These calculations were made for $\nu = 0.25$ and some small variation may be expected for other values of Poisson's ratio. With increasing depth h the shear stresses at the rigid base decrease as shown by the relative values when h = b and h = 5b. In the lower diagram of Figure 9, the depth of the layer is indicated by the vertical scale and two S_1 stress curves are shown for h = a and h = 5b, the latter being considerably distorted in comparison with

---

wishes to acknowledge an error pointed out by the writer. There should be a negative sign (rather than positive) in the term $\sinh^2 a$ in the definition of M at the end of page 38. Subsequent formula should be altered accordingly with a rearrangement of curves C and D in Figure 2 of his paper.

[11] By translating the x axis to the top of the surface with $y' = h - y$, then

$$\underset{h\to\infty}{\text{Limit}}\, p_x = \int_0^\infty Q(a)e^{-ay'}(ay' - 1)a^2\cos ax\,da.$$

A similar result holds for p_y. These are Boussinesq results for symmetrical loads.

the former. If the vertical scale were enlarged to the proper ratio, the curve representing the case h=5b would resemble the S_1 curve of Figure 2, except that the initial values at the top surface

SURFACE DEFLECTION FOR A FINITE LAYER

Employing the last of Eqs. (11) one obtains a general displacement function. At the top surface this becomes

$$(19) \qquad Ev\Big|_{y=h} = -2(1-\nu^2)\int_0^\infty \frac{Q(a)}{\Delta}\,[(3-4\nu)\cosh ah \sinh ah - ah]\,a\cos ax\,da.$$

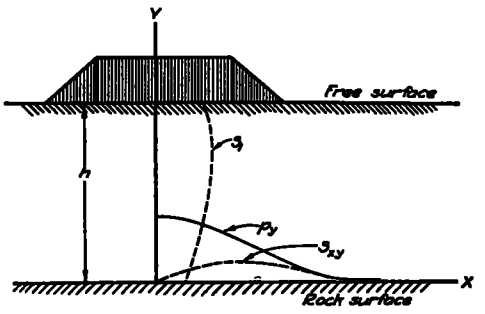

Figure 8

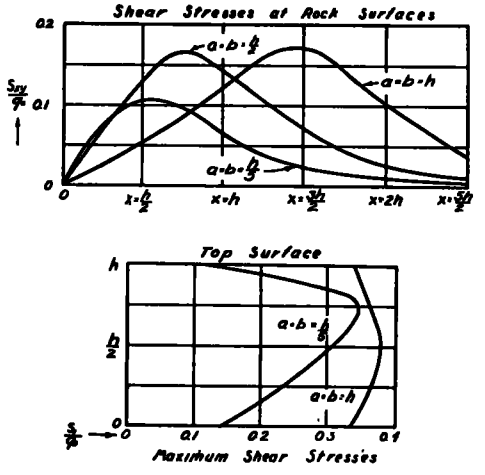

Figure 9

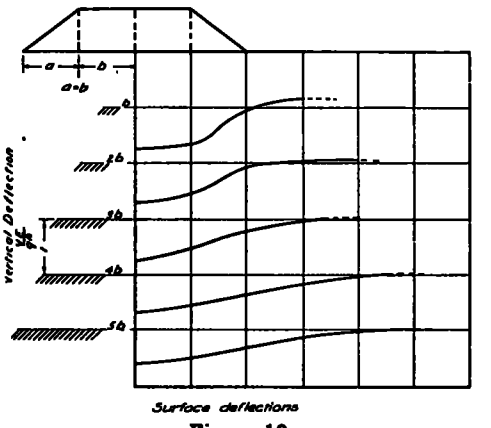

Figure 10

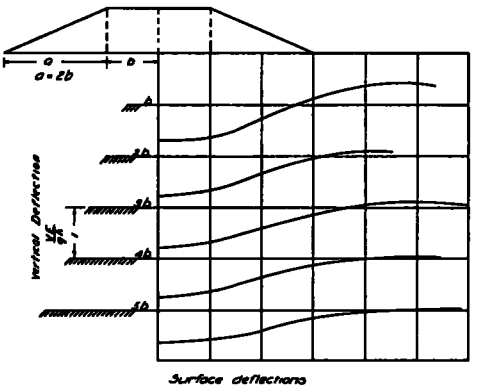

Figure 11

are not zero as in the infinite layer. This means that p_y and p_x are not equal directly under the load when the layer is finite, their difference increasing with decreasing depth of elastic layer. The maximum value of S_1 is much greater than S_{xy} at the base and one may expect shearing failure within the layer before similar failure occurs at the rock surface.

For a symmetrical trapezoidal loading $Q(a)$ is given by Eq. (16). For $\nu=0.25$ a series of the surface deflection curves are shown in Figures 10 and 11 for two different types of loads and for five increasing depths of layer. At the left of the vertical axis of symmetry the depth of the layer is shown and the scale indicates that for each layer the deflection is

given in terms of the height of that layer. For example in Figure 11 when h=3b the maximum value is vE/q=0.73h, and when h=4b, vE/q=0.65h. With increasing depth of layer the deflections continue to increase and the point of zero surface deflection recedes farther from the loading. This confirms the results of

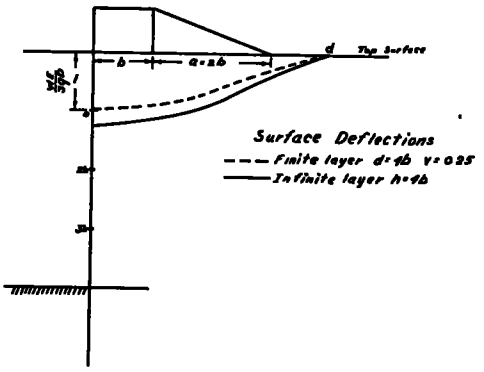

Figure 12

the infinite layer in which as the value d increased the deflections increased. Whereas the value of d was indeterminate, and only local relative deflections could be found in the infinite layer, the complete deflection surface for the finite layer can be determined. These latter curves do not oscillate with alternate positive and negative deflections. The extreme right portions of the curves of Figures 10 and 11 decay asymptotically along the horizontal. A comparison of the curve d=4b from Figure 11 and the lowest curve of Figure 5a is made in Figure 12.

SUMMARY

In this paper the stresses and surface deflections of a semi-infinite elastic medium and of an elastic layer of finite depth are obtained by the principle of superposition. In the first part of the paper the author determines the stresses induced in a supporting medium for surface loads which simulate triangular, rectangular, symmetrical and unsymmetrical trapezoidal surface loads. In particular it is shown that the depth at which the maximum principal shear occurs is at a depth approximately equal to one-half of the length of an equivalent rectangular load of equal intensity. This maximum shear value does not exceed 0.318q where q is the maximum intensity of the surface loading.

Only the relative surface deflection due to these loads can be determined. Two undetermined parameters remain to be found by experiment. One of these is $E'=E/(1-\nu^2)$ where E is the elastic compression modulus and ν is Poisson's ratio. Since this parameter appears only as a scale factor in the deflection, it may be designated as a foundation modulus. The second parameter capable of experimental determination is a distance d which locates a surface point having no displacement and relative to which all other surface deflections are referred.

In the second part of the paper, the stresses and surface deflection are determined for an elastic layer of finite depth supported on a rough rigid base. It is shown that the stresses are no longer independent of Poisson's ratio ν, and that shearing failure occurs within the layer before it occurs at the supporting base. Using $\nu=0.25$ the surface deflections are evaluated for several types of surface loading and varying depths of the elastic layer. All the results of the first part of the paper may be derived as a limiting case by allowing the depth h of the layer to become infinite.

APPENDIX *

The stresses p_y, p_x, and S_{xy} for the loading of Figure 3d can be obtained by summation of elemental loads employing Eqs. (1). The only change in the present case is that the angle θ is measured from

* The writer wishes to acknowledge the assistance of Mr. R. H. Tripp, graduate student at Iowa State College, in obtaining the equations in this appendix.

the direction of the loading which is no longer normal to the inclined surface plane. The results of Figure 3d may be obtained by superposing the results for triangular and parallelogram loads. The loading OAC of Figure 13 is equivalent to loads OAB+ABCD−ACD. This is permissible since it is assumed that the vertical intensity of the loading on the inclined surface is given by the configuration OACB.

zontal surface plane when k=0, that is,

$$p_y=\frac{-q_0}{2b\pi}(x_1a_1-2b\sin\theta_2\cos\theta_2),$$

$$p_x=p_y+\frac{q_0h}{b\pi}\log R_1/R_2, \tag{21}$$

$$S_{xy}=\frac{q_0}{2b\pi}(a_1h-2b\cos^2\theta_2).$$

With the notation of Figure 14 the stresses due to the parallelogram loading ABCD are

$$p_y=\frac{q_0}{\pi(1+k^2)^2}\Big[k(1+k^2)(\sin^2\theta_2-\sin^2\theta_1)+\frac{(1+k^2)}{2}(\sin2\theta_2-\sin2\theta_1)$$
$$-a_1(1+3k^2)-2k^2\log R_1/R_2\Big],$$

$$p_x=\frac{2q_0}{\pi(1+k^2)}\left[k\log\frac{R_2}{R_1}-a_1\right]-p_y, \tag{22}$$

$$S_{xy}=\frac{q_0}{\pi(1+k^2)^2}\Big[(1+k^2)(\sin^2\theta_2-\sin^2\theta_1)-\frac{k(1+k^2)}{2}(\sin2\theta_2-\sin2\theta_1)$$
$$-a_1k(1-k^2)-2k^2\log R_1/R_2\Big].$$

With the notation of Figure 13 the cases of a triangular load OAB on an inclined surface is given in the following equations.

Triangle OAB:

$$p_y=\frac{q_0}{b\pi(1+k^2)^3}\Big\{b(1+k^2)\Big[\frac{1+k^2}{2}\sin2\theta_2-k(1+\cos^2\theta_2)+k^2\sin^2\theta_2\Big]$$
$$-\frac{a_1}{2}\Big[(1+6k^2-3k^4)x_1+2h(3k^2-k)\Big]$$
$$+2bk^2(1+k^2)-k^2[4kx_1-h(3-k^2)]\log R_1/R_2\Big\},$$

$$p_x=\frac{q_0}{b\pi(1+k^2)^2}\Big\{[(1-k^2)h-2kx_1]\log R_1/R_2+2bk(1+k^2)$$
$$-a_1[(1-k^2)x_1+2kh]\Big\}-p_y, \tag{20}$$

$$S_{xy}=\frac{q_0}{b\pi(1+k^2)^3}\Big\{b(1+k^2)\Big[(1+k^2)\sin^2\theta_2-\frac{k(1+k^2)}{2}\sin2\theta_2-(1-k^2)\Big]$$
$$-\frac{a_1}{2}[2kx_1(1-3k^2)-h(1-6k^2+k^4)]$$
$$+2bk^2(1+k^2)-[k^2x_1(3-k^2)-2kh(1-k^2)]\log R_1/R_2\Big\},$$

where k=tanα (not to be confused with k of Eqs. (3)).

These formulas provide the results for a rectangular load on a horizontal surface plane when k=0.

To obtain the stresses p_t, p_n, S_{tn} (indicated in Figure 14) which are parallel and normal to the inclined surface plane one employs the equations

$$p_t=p_x\cos^2\alpha+p_y\sin^2\alpha+2S_{xy}\sin\alpha\cos\alpha,$$
$$p_n=p_x\sin^2\alpha+p_y\cos^2\alpha-2S_{xy}\sin\alpha\cos\alpha, \tag{23}$$
$$S_{tn}=(p_y-p_x)\sin\alpha\cos\alpha+S_{xy}(\cos^2\alpha-\sin^2\alpha).$$

Equations (20) reduce to known results [2] for a right triangle load on a hori-

With Eqs. (23) one may show that both the normal stress p_n and the tan-

gential stress S_{tn} vanish at the surface when external to the load and yield the correct values under the load. These values are

For parallelogram:

$$p_n = -q_0 \cos\alpha, \quad S_{tn} = -q_0 \sin\alpha \cos\alpha,$$

For triangle:

$$p_n = -\frac{q_0 x_1}{2b} \cos^2 \alpha, \quad S_{tn} = -\frac{q_0 x_1}{2b} \sin\alpha \cos\alpha.$$

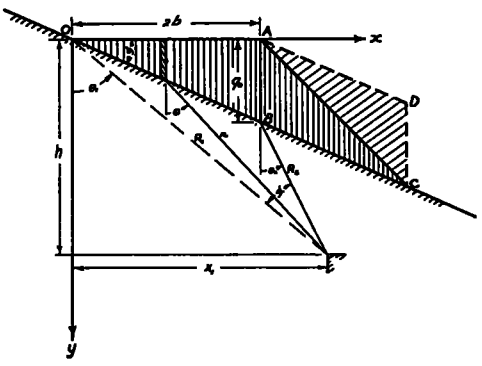

Figure 13

The tangential stress p_t along the surface plane changes from a compressive stress to a tensile stress at some point under the loading. In the case of the parallelogram this point depends only on the slope of the surface plane, and in the triangle loading it also depends upon the length of loading 2b.

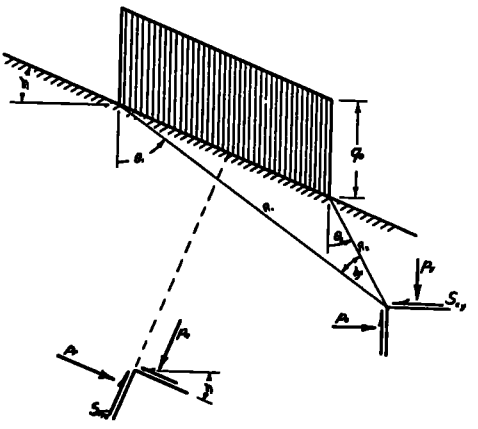

Figure 14

DISCUSSION ON SHEARING STRESSES AND SURFACE DEFLECTIONS DUE TO TRAPEZOIDAL LOAD

MR. L. A. PALMER, *Public Roads Administration:* The author has followed a general procedure which is as old as soil mechanics and which "neglects" the fact that stresses within the embankment and supporting soil may be more or less continuous. This apparent "neglect" is necessary if any sort of mathematical expressions for stress are to be obtained. One must consider the load due to a fill or embankment simply as a load and not as a projection of the undersoil. In a natural earth embankment this procedure may not be warranted.

It may be true that the stress trajectories within a finite earth mass, such as a fill, and those in the "infinite" soil mass, the supporting earth, are more or less continuous but to assume anything with respect to such continuity is almost useless. Therefore, this writer is in thorough agreement with the author's procedure. It would be well for those who object to this procedure to suggest a better one in some detail.

For soils that consolidate due to slow egress of water under a foundation load, it has apparently been customary in soil mechanics to take μ, Poisson's ratio, as $\frac{1}{2}$. No defense of this procedure is at present offered. Let S denote the total subsidence due to all causes, S_L the settlement due to distortion at constant volume with $\mu = \frac{1}{2}$, and S_C the settlement due to consolidation with $\mu = 0$. Then

$$S = S_L + S_C.$$

With reference to Figure 4 of the

author, the vertical displacement, w, at any point on the axis of symmetry may be shown to be

$$w = \frac{yp}{\pi Ea}\left[\frac{y^2}{2}\log_e\frac{\sqrt{y^2+(a+b)^2}}{\sqrt{y^2+b^2}} + \frac{(a+b)^2}{2}\log_e\frac{\sqrt{y^2+(a+b)^2}}{a+b} - \frac{b^2}{2}\log_e\frac{\sqrt{y^2+b^2}}{b}\right] + \text{constant.}$$

The value of the constant is obtained by giving a value to y of magnitude such that $w=0$ for practical purposes. For $y=0$, $w=Wmax=S_L=$the constant.

A more general expression for w for any point in the supporting earth and for any value of μ but which contains a constant instead of the author's "d" is easily derivable.

DR. KARL TERZAGHI: In the first part of the paper, dealing with the case illustrated by Figure 3d, the general reader would undoubtedly appreciate the inclusion of the Boussinesq equations for the stresses due to a force acting in the direction of the plane surface of a semi-infinite elastic medium, because these equations are not as well known as the equations pertaining to load perpendicular to the surface.

The last part of the paper (elastic layer on a rigid rock base) deals with a very difficult problem. The following solutions may be mentioned.

E. Melan, "Die Verteilung des Druckes durch eine elastische Schichte," *Beton u. Eisen,* 1919. Point and line load, no bond between layer and base.

K. Marguerre, "Druckverteilung durch eine elastische Schichte auf starrer, rauher Unterlage," Ingenieur Archiv, 1931. Line load, perfect bond between layer and base.

W. Passer, "Druckverteilung durch eine elastische Schichte." Sitzber. Ak. Wiss., Wien, Abt. IIa, Vol. 144, 1935. Point load, perfect bond between layer and base.

M. A. Biot, "Effect of Certain Discontinuities on the Pressure Distribution in a Loaded Soil," *Physics,* Dec. 1935. Point and line load, no bond and perfect bond.

None of these very competent investigators attempted to accomplish more than a computation of the distribution of the stresses over the rigid bottom. Yet their investigations are rather involved. The results contained in the paper by Mr. Holl go far beyond this modest accomplishment. Therefore the reader is naturally interested in the details of the mathematical investigations which led to the results.

The value of the paper could also be increased by references such as those mentioned above.

DR. HOLL: As stated in the paper, one has the alternative of referring the relative deflections to a surface point or to an internal point having no deflection. Mr. Palmer has given such an expression referring the deflection to an internal point on the axis of symmetry and for the special value μ (or ν) $=0.50$. The author's choice of referring the relative deflections to a surface point d was based upon the fact that surface deflections admitted experimental verification.

The references and mathematical derivations alluded to by Dr. Terzaghi were omitted from the abbreviated preprint. The author acknowledged these omissions at the presentation of the paper and explained the relationship of the plane deformation analysis of this paper to the problems of plane stress and axially symmetric stress situations of the quoted references.